Negative plasma potential relative to electron-emitting surfaces

M. D. Campanell*
Princeton Plasma Physics Laboratory, Princeton University, Princeton, New Jersey 08543, USA
(Received 19 June 2013; published 9 September 2013)

Most works on plasma-wall interaction predict that with strong electron emission, a nonmonotonic "space-charge-limited" (SCL) sheath forms where the plasma potential is positive relative to the wall. We show that a fundamentally different sheath structure is possible where the potential monotonically increases toward a positively charged wall that is shielded by a single layer of negative charge. No ion-accelerating presheath exists in the plasma and the ion wall flux is zero. An analytical solution of the "inverse sheath" regime is demonstrated for a general plasma-wall system where the plasma electrons and emitted electrons are Maxwellian with different temperatures. Implications of the inverse sheath effect are that (a) the plasma potential is negative, (b) ion sputtering vanishes, (c) no charge is lost at the wall, and (d) the electron energy flux is thermal. To test empirically what type of sheath structure forms under strong emission, a full plasma bounded by strongly emitting walls is simulated. It is found that inverse sheaths form at the walls and ions are confined in the plasma. This result differs from past particle-in-cell simulation studies of emission which contain an artificial "source sheath" that accelerates ions to the wall, leading to a SCL sheath at high emission intensity.

DOI: 10.1103/PhysRevE.88.033103 PACS number(s): 52.40.Kh, 52.65.−y, 52.40.Hf

I. INTRODUCTION

Plasma-wall interaction (PWI) is critical for plasma applications [1]. Bombardment by plasma ions heats the wall and can sputter away wall atoms. Sputtering not only erodes the wall but also contaminates the plasma with unwanted impurities. Bombardment by plasma electrons further heats the wall, increasing the risk of melting. Even in low-temperature plasma devices where the walls may not be severely damaged, the PWI is still important; the properties of the plasma itself depend on balances between heating and ionization vs the losses of energy and charged particles at the walls. The potentials of the walls relative to the plasma and to other walls are important quantities in laboratory and space systems.

For a "floating" wall which draws zero net current in equilibrium, the net electron flux must equal the ion flux,

$$\Gamma_{e,\mathrm{net}} = \Gamma_\mathrm{p} - \Gamma_\mathrm{emit} = \Gamma_\mathrm{ion}. \quad (1)$$

The plasma electron influx Γ_p is a function of wall potential relative to the plasma, Φ. Γ_ion is determined by plasma properties and the Bohm criterion, independently of Φ [2,3]. Generally $\Gamma_{\mathrm{p}0} \equiv \Gamma_\mathrm{p}(\Phi = 0) \gg \Gamma_\mathrm{ion}$, so when there is no emission, the floating potential Φ_f must be sufficiently negative to reflect away most electrons approaching the wall, satisfying $\Gamma_\mathrm{p}(\Phi_\mathrm{f}) = \Gamma_\mathrm{ion}$. The potential profile $\varphi(x)$ takes the form of a monotonic classical Debye sheath, drawn qualitatively in Fig. 1.

Electron emission from the walls can play an important role in plasma-wall interaction. From (1), it is clear that emission forces more plasma electrons to reach the wall to balance Γ_ion. Hence emission leads to reduction of $|\Phi_\mathrm{f}|$, reduced ion impact energies, enhanced electron energy flux to the walls, and cooling of the plasma by the cold emitted electrons. These effects are known to be important in numerous applications including fusion machines [1,4].

A particularly interesting and important question is what happens when a wall emits more electrons than it collects from the plasma. If $\Gamma_\mathrm{emit} > \Gamma_\mathrm{p}$, Eq. (1) cannot be satisfied because Γ_ion cannot be negative. This problem can arise when the secondary electron emission (SEE) coefficient of the plasma electrons, γ, exceeds unity for the wall material; this is known or predicted to occur in certain conditions at surfaces in tokamak scrape-off layers [5,6], plasma thruster channels [7], dusty plasmas [8], and hot astrophysical plasmas [9]. When $\gamma > 1$, $\Gamma_\mathrm{emit} = \gamma\Gamma_\mathrm{p} > \Gamma_\mathrm{p}$ for any Φ.

It is also possible to have $\Gamma_\mathrm{emit} > \Gamma_\mathrm{p}$ at surfaces emitting a thermionic or photoelectron current that exceeds the electron saturation current $\Gamma_{\mathrm{p}0}$, the maximum possible Γ_p. Examples include heated cathodes [10], emissive probes [11], and sunlit objects in space plasmas [9]. In this paper, we will treat the "strong emission problem" in terms of SEE coefficients, although the results apply without loss of generality to other emission types.

Most papers on PWI with emission predict that when $\gamma > 1$, a "space-charge-limited" (SCL) sheath forms [12–16], as illustrated in Fig. 1. In theory, a potential "dip" can reflect enough of the emission back to the wall to maintain zero net current. But we will show that the "inverse sheath" in Fig. 1 is also possible. The inverse sheath regime has some important features that differ from the familiar classical and

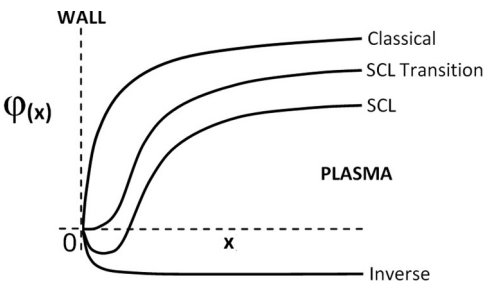

FIG. 1. Qualitative drawings of the potential relative to the wall in the classical (monotonic, Φ_f negative), SCL (nonmonotonic, Φ_f negative), and inverse (monotonic, Φ_f positive) sheath regimes.

*michaelcampanell@gmail.com

SCL regimes. (a) The plasma potential is negative relative to the wall ($\Phi_f > 0$). (b) Ions are confined, so no wall sputtering or loss of charged particles from the plasma occurs. (c) No ion-accelerating presheath structure exists in the plasma interior. (d) The electron influx is the maximum thermal value Γ_{p0}. In light of these features, it is worthwhile to consider the inverse sheath concept in detail.

In Sec. II, we discuss the physical origin of the different sheath structures in Fig. 1 and explain why the inverse sheath was not captured in past theoretical studies of emission. In Sec. III, a mathematical model proving the existence of the inverse sheath solution when $\gamma > 1$ under general conditions is presented. Simple estimates of the potential amplitude and spatial width of the inverse sheath are derived. In Sec. IV, the implications of the inverse sheath effect for PWI are elaborated. In Sec. V, we investigate whether inverse sheaths or SCL sheaths are more likely to form in practice under strong emission. A particle simulation is presented and the sheath physics is analyzed. Lastly, Sec. VI contains a conclusion summarizing the results.

II. SHEATH STRUCTURE VARIATION WITH EMISSION INTENSITY

A. General considerations

In this section, we will analyze why each sheath structure in Fig. 1 can exist, and under what conditions. The discussion is kept conceptual in order to focus on the physical meaning that is not obvious in mathematical derivations. We will reconsider the fundamental assumptions inherent in conventional sheath theories to see why the common assumption of $\Phi_f < 0$ can be violated with emission. Note that throughout this paper Φ is defined as $\varphi(\text{wall}) - \varphi(\text{plasma})$, so it is independent of where the reference potential is.

Consider an unmagnetized planar plasma with Maxwellian electrons and cold ions in contact with a nonemitting floating wall. Due to the electron thermal motion it can safely be assumed that in equilibrium, the wall must be negatively charged, and ions will be attracted to the wall. Because the distant plasma must be shielded from the negative wall, the ion density must fall off more slowly than the electron density as the wall is approached, so that the net space charge near the wall is positive. From these assumptions, the Bohm criterion for the ion velocity into the sheath is derivable, which implies the necessity for a large presheath structure to accelerate ions [2,3]. The Bohm criterion along with the presheath solution essentially fixes Γ_{ion} at the sheath edge, independently of Φ. In equilibrium, Φ_f must be sufficiently negative to maintain $\Gamma_p(\Phi_f) = \Gamma_{ion}$. The exact Φ_f can be calculated, and then the full sheath structure can be derived if desired. The charge density distributions for a nonemitting classical Debye sheath are plotted qualitatively in Fig. 2(a).

With electron emission, a few changes occur. For $\gamma > 0$, the floating potential amplitude $|\Phi_f|$ is reduced from the zero-current condition $\Gamma_p(\Phi_f) = \Gamma_{ion}/(1-\gamma)$. Emitted electrons contribute to the electron charge density distribution; see Fig. 2(b). The contribution is largest near the wall because emitted electrons start with small initial velocities and acquire higher velocities further from the wall via sheath acceleration.

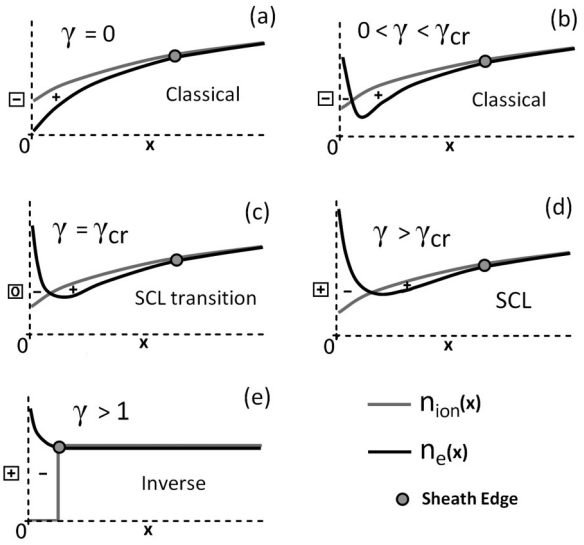

FIG. 2. Qualitative plots of the electron and ion density distributions near the wall for different γ values. The sheath structure corresponding to each charge distribution is indicated (cf. Fig. 1). The sign of the wall charge is marked in the square boxes. In (b)–(d), there are two oppositely charged layers in the sheath. The combined charge of the two layers is positive in (b), zero in (c), and negative in (d).

For small γ, the negative charge layer in the sheath is smaller in magnitude than the positive layer, so the wall charge still must be negative and the potential must increase outward from the wall. Hence the sheath structure remains qualitatively the same as the classical Debye sheath in Fig. 1.

As γ approaches unity, the emission flux increases sharply, $\Gamma_{emit} = \gamma\Gamma_{ion}/(1-\gamma)$. For some critical γ_{cr} below unity, the electron charge in the sheath will equal the ion charge; see Fig. 2(c). At this point the wall charge must be zero for the distant plasma to be shielded. The result is the "transition" sheath in Fig. 1, where the electric field vanishes at the wall. For any further increase in γ, the total charge in the sheath will be negative [Fig. 2(d)], so the wall charge must be positive. Therefore $\varphi(x)$ is nonmonotonic for $\gamma_{cr} < \gamma < 1$, taking the shape of the SCL sheath in Fig. 1. Although the wall charge is positive in the SCL regime, the *combined* charge of the wall and the negative space charge layer is negative. The positive charge layer further inward shields the plasma, meaning that the same Bohm criterion [2,3] must still be met at the sheath edge, and a presheath must exist to accelerate the ions.

The SCL sheath structure remains a mathematically valid solution for $\gamma > 1$. In the SCL regime, there is an influx of emitted electrons Γ_{ref} that reflect in the potential dip and return to the wall. So even if the term $\Gamma_p - \Gamma_{emit} = \Gamma_p(1-\gamma)$ is negative, zero current can be maintained by an SCL sheath if the dip amplitude is sufficient so that

$$\Gamma_{e,net} = \Gamma_p(1-\gamma) + \Gamma_{ref} = \Gamma_{ion}. \quad (2)$$

However, note that when $\gamma > 1$, Eq. (2) could be satisfied even with $\Gamma_{ion} = 0$. One could propose that a fundamentally different type of sheath solution should exist where $\Phi_f > 0$, as sketched in Fig. 1. When $\Phi_f > 0$, the ions are confined and the wall draws the full thermal electron influx from the plasma

($\Gamma_p = \Gamma_{p0}$). Some of the emitted electrons will be reflected back to the wall. If Φ_f is sufficiently positive so that $\Gamma_{ref} = \Gamma_{p0}(\gamma - 1)$, zero current is maintained. A formal derivation of the inverse sheath solution will be presented in Sec. III. We will find that the charge density profiles appear as sketched in Fig. 2(e).

B. Comparison to past theoretical models of plasma-wall interaction with emission

The possibility of an emissive plasma sheath with $\Phi_f > 0$ has been unexplored in the literature. It is well known that such a sheath arises at emitting surfaces in vacuum [17], but in plasmas it is widely predicted that $\Phi_f < 0$ for all emission intensities.

Hobbs and Wesson presented the pioneering theoretical treatment of PWI with SEE [12]. They solved Poisson's equation in the sheath using Boltzmann plasma electrons, cold ions, and cold emitted electrons. They showed that the electric field at the floating wall drops to zero when γ reaches a critical value γ_{cr} below unity (SCL transition sheath). Other researchers have since considered the influence of the kinetic correction to the electron velocity distribution in the sheath [13,16,18], nonzero ion temperature [13], nonzero emitted electron temperature [16], current-carrying surfaces [18], the presence of incident electron beams [19], and supermarginal Mach numbers [15] on emissive sheath structures.

In each of the aforementioned treatments [12,13,15,16,18,19], it is explicit in the model that ions enter the sheath with a (Bohm) flow velocity, and the charge densities are written in terms of a $\varphi(x)$ that is assumed below the sheath edge potential everywhere in the sheath. The case of $\gamma > 1$ is not derived mathematically because of the complexities inherent in handling a nonmonotonic $\varphi(x)$; usually the transition sheath with $\gamma = \gamma_{cr}$ is modeled by requiring the electric field to vanish at the wall [12,15,16]. But in most papers it is stated or implied that for all $\gamma > \gamma_{cr}$, a SCL-type sheath will form. Hobbs and Wesson wrote "For $\gamma > \gamma_{cr}$, no monotonic solution for $\varphi(x)$ exists and a potential well forms such that a fraction of the emitted electrons are returned to the wall in order to maintain the effective γ equal to γ_{cr}. Under these conditions the emission current is space-charge limited."

Overall, we see that the conventional models of PWI with SEE conclude that a SCL sheath forms under strong emission because it is the only possible solution under their assumptions that $\Phi_f < 0$ and/or that ions flow to the wall (either assumption also implies the other). The assumptions are also present in Langmuir's seminal work on cathode sheaths with thermionic emission [20]. He stated that emission cannot change Γ_{ion} "for this is fixed by the plasma," and concluded that a nonmonotonic "double sheath" forms under strong emission. Interestingly, a sheath solution where $\varphi(x)$ monotonically increases from the sheath edge to a strongly emitting wall was claimed in a few PWI models by Sizonenko [21] and by Morozov and Savel'ev [22]. But even in their works, the authors still assumed that ions entered the sheath with a substantial flow velocity and reached the wall. A presheath would have to accelerate ions into the sheath for such a structure to exist. The full potential profile must be nonmonotonic and Φ_f must still be negative.

It is the ion flow assumption that can break down under strong emission. As discussed in Sec. II A, the assumption originates from classical sheath theory without emission, where it can safely be assured that ions flow to the negatively charged wall. The Bohm criterion on the minimum ion flow velocity is a separate subsequent requirement for the formation of the positive shielding charge [2,3]. But with emission, we saw that an ion wall flux only remains necessary for current balance in the range $\gamma < 1$, where the term $\Gamma_p(1-\gamma)$ in (2) is positive, requiring Γ_{ion} to be nonzero. When $\gamma > 1$, because the wall must be positively charged to suppress some of the emission, it is also unnecessary to keep the Bohm criterion because a positively charged wall can be shielded by a *single* layer of negative charge, as in Fig. 2(e). In the next section, we will find that the $\Phi_f > 0$ sheath solution arises naturally if the assumption of ion flow at the sheath edge is lifted.

III. STRUCTURE OF AN INVERSE SHEATH

A. Overview

The result that the inverse sheath potential profile can maintain zero current with $\Gamma_{ion} = 0$ when $\gamma > 1$ by suppressing the "extra emission" seems intuitive. However, showing that the inverse sheath can exist requires proving that it is self-consistent with the corresponding charge density profiles.

Suppose $\varphi(x)$ is flat in the neutral plasma interior and starts increasing monotonically from the sheath edge to the wall, as in Fig. 1. Assuming that the plasma ions are cold and nonflowing, the ions cannot climb to a higher potential. Therefore, the ion density is zero in the sheath, as in Fig. 2(e). It follows that the charge density will be negative everywhere in the sheath (plasma electrons flow freely to the wall and clearly produce a nonzero density everywhere). Hence, from Poisson's equation, $\varphi(x)$ will monotonically increase from the edge to the wall. If the wall is charged positively to balance the negative charge in the sheath, the plasma will be shielded and $\varphi(x)$ can indeed be flat interior to the sheath edge.

We conclude that the requisite charge density profiles can exist self-consistently with the potential profile structure. To more closely investigate properties of the inverse sheath such as its spatial size and potential amplitude, we will present an analytical model.

B. Mathematical model

Consider an unmagnetized planar plasma contacting a floating wall with a given $\gamma > 1$. Let Φ_{-1} denote the positive wall potential relative to the sheath edge; see Fig 3. Let N designate the neutral plasma density at the edge. Assuming the ions are cold, the ion density N_{ion} drops abruptly from N to zero at the edge; cf. Fig. 2(e). The electron density N_e in the inverse sheath consists of three distinct components, one corresponding to each flux component in Fig. 3.

Let us assume that the thermal plasma electrons approaching the wall have a half-Maxwellian distribution of temperature T_p, starting with density N_p^{SE} at the edge. The plasma electrons accelerate through the inverse sheath toward

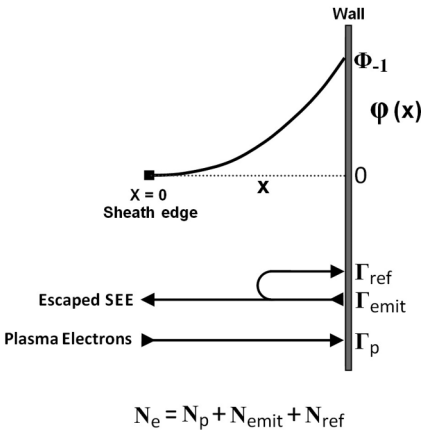

FIG. 3. Parameters and notations used for the analytical inverse sheath model. The sheath is assumed to be collisionless.

the wall, producing a density in terms of φ given by

$$N_{\rm P}(\varphi) = N_{\rm P}^{\rm SE} \exp\left(\frac{e\varphi}{T_{\rm p}}\right) \mathrm{erfc}\left(\sqrt{\frac{e\varphi}{T_{\rm p}}}\right). \tag{3}$$

Suppose the secondaries are emitted with a half-Maxwellian distribution of temperature $T_{\rm emit}$, starting with a density $N_{\rm emit}^{\rm wall}$ at the wall. The density of secondaries traveling away from the wall under the retarding force is expressible by a Boltzmann factor,

$$N_{\rm emit}(\varphi) = N_{\rm emit}^{\rm wall} \exp\left(\frac{e(\varphi - \Phi_{-1})}{T_{\rm emit}}\right). \tag{4}$$

All secondaries emitted with kinetic energy normal to the wall exceeding $e\Phi_{-1}$ will escape the inverse sheath. The rest will reflect back to the wall. The charge density at each point from reflected secondaries is

$$N_{\rm ref}(\varphi) = N_{\rm emit}^{\rm wall} \exp\left(\frac{e(\varphi - \Phi_{-1})}{T_{\rm emit}}\right) \mathrm{erf}\left(\sqrt{\frac{e\varphi}{T_{\rm emit}}}\right). \tag{5}$$

Equations (3)–(5) can be formally derived by using the Vlasov equation to solve for the velocity distribution functions in the sheath in terms of φ, accounting for the cutoff velocities, and then integrating the distributions to get the densities. We omit the details because similar expressions are ubiquitous in sheath theories where half Maxwellians are accelerated, decelerated, and reflected. For instance, the emitted and reflected secondaries in Eqs. (4) and (5) are respectively analogous to incident and reflected plasma electrons in a classical sheath (cf. Ref. [18]).

So far, $N_{\rm P}^{\rm SE}$ and $N_{\rm emit}^{\rm wall}$ in (3)–(5) are unspecified quantities which should be expressed in terms of the known N. The condition for neutrality of the plasma must account for the charge density from secondaries that escape the inverse sheath,

$$N_{\rm P}^{\rm SE} + N_{\rm emit}^{\rm SE} = N. \tag{6}$$

The secondary electron density at the edge, $N_{\rm emit}^{\rm SE}$, is expressible in terms of $N_{\rm emit}^{\rm wall}$ via (4) with $\varphi = 0$:

$$N_{\rm emit}^{\rm SE} = N_{\rm emit}^{\rm wall} \exp\left(\frac{-e\Phi_{-1}}{T_{\rm emit}}\right). \tag{7}$$

$N_{\rm emit}^{\rm wall}$ and $N_{\rm P}^{\rm SE}$ can be linked through γ. The plasma electron influx is the full thermal flux of the half-Maxwellian source, $\Gamma_{\rm p} = \Gamma_{\rm p0} = N_{\rm P}^{\rm SE}(2T_{\rm p}/m_e\pi)^{1/2}$. The emitted flux from the wall is $\Gamma_{\rm emit} = N_{\rm emit}^{\rm wall}(2{\rm T}_{\rm emit}/m_e\pi)^{1/2}$. Then because $\Gamma_{\rm emit} = \gamma\Gamma_{\rm p0}$, we have

$$N_{\rm emit}^{\rm wall}\sqrt{T_{\rm emit}} = \gamma N_{\rm P}^{\rm SE}\sqrt{T_{\rm p}}. \tag{8}$$

Now to determine Φ_{-1}, we use the zero-current condition, $\Gamma_{\rm p} - \Gamma_{\rm emit} + \Gamma_{\rm ref} = 0$. With $\Gamma_{\rm p} = \Gamma_{\rm emit}/\gamma$ it follows that

$$\Gamma_{\rm ref} = \frac{\gamma - 1}{\gamma}\Gamma_{\rm emit}. \tag{9}$$

In terms of $\Gamma_{\rm emit}$, the flux of the half-Maxwellian secondaries that escape past the inverse sheath barrier is $\Gamma_{\rm emit}\exp(-e\Phi_{-1}/T_{\rm emit})$. So $\Gamma_{\rm ref}$ is just the complement,

$$\Gamma_{\rm ref} = \Gamma_{\rm emit}\left[1 - \exp\left(\frac{-e\Phi_{-1}}{T_{\rm emit}}\right)\right]. \tag{10}$$

Equating (9) with (10) yields a simple expression for the inverse sheath amplitude Φ_{-1}:

$$e\Phi_{-1} = T_{\rm emit}\ln\gamma. \tag{11}$$

Now plugging (11) into (7) and solving Eqs. (6)–(8) for $N_{\rm P}^{\rm SE}$ and $N_{\rm emit}^{\rm wall}$ gives

$$N_{\rm P}^{\rm SE} = \frac{N}{1 + \sqrt{T_{\rm p}/T_{\rm emit}}}, \tag{12}$$

$$N_{\rm emit}^{\rm wall} = \frac{\gamma N\sqrt{T_{\rm p}/T_{\rm emit}}}{1 + \sqrt{T_{\rm p}/T_{\rm emit}}}. \tag{13}$$

Summing Eqs. (3)–(5) where Φ_{-1}, $N_{\rm P}^{\rm SE}$, and $N_{\rm emit}^{\rm wall}$ are defined in (11)–(13), gives the total electron density in the inverse sheath, $N_e = N_p + N_{\rm emit} + N_{\rm ref}$ in terms of φ.

C. Discussion and application of the model

The exact potential profile solution $\varphi(x)$ and corresponding $N_e(x)$ for a given $\{N, T_{\rm p}, T_{\rm emit}, \gamma\}$ can be calculated by solving Poisson's equation numerically using the expression for $N_e(\varphi)$ derived above. We will show in this section that the essential properties of the inverse sheath can be described in simple terms analytically.

One important property of the inverse sheath is that its amplitude is very small compared to classical and SCL sheaths in hot plasmas. Classical and SCL sheaths always have amplitudes $\geqslant \sim T_{\rm p}$. On the other hand, the inverse sheath amplitude $T_{\rm emit}\ln(\gamma)$ is determined by $T_{\rm emit}$ no matter how large is $T_{\rm p}$. Although γ itself varies with $T_{\rm p}$ if the emission type is SEE, the function $\gamma(T_{\rm p})$ has a maximum less than 2 for most materials [23]. So in general for SEE, $e\Phi_{-1} < T_{\rm emit}$.

To investigate the electron density, we insert $e\varphi = e\Phi_{-1} = {\rm T}_{\rm emit}\ln(\gamma)$ into the formula for $N_e(\varphi)$ to give an expression for the total electron density at the wall interface, $N_e^{\rm wall}$. We write $N_e^{\rm wall}$ in terms of the dimensionless $T_{\rm R} \equiv T_{\rm p}/T_{\rm emit}$ because only the temperature ratio appears in the expression,

$$N_e^{\rm wall} = N\frac{\gamma^{1/T_{\rm R}}\mathrm{erfc}\left(\sqrt{\frac{\ln\gamma}{T_{\rm R}}}\right) + \gamma\sqrt{T_{\rm R}}[1 + \mathrm{erf}(\sqrt{\ln\gamma})]}{1 + \sqrt{T_{\rm R}}}. \tag{14}$$

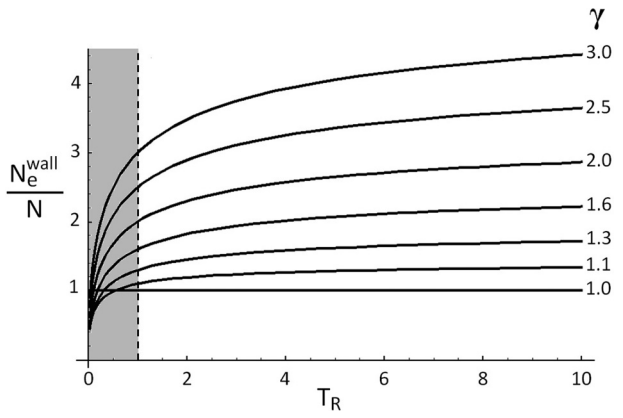

FIG. 4. Variation of N_e^{wall} with γ and $T_R \equiv T_p/T_{\text{emit}}$. N_e^{wall} is normalized to the sheath edge plasma density N. The range $T_R < 1$ is unrealistic but is included for completeness.

In Fig. 4, we plot N_e^{wall} vs T_R for various γ values. We focus on the range $T_R > 1$ because only this range is of much practical interest. T_{emit} for various emission types is only a few eV or less [16,24]. For plasmas hot enough to induce $\gamma > 1$ from a typical material, T_p is from tens to hundreds of eV [23]. While thermionic or photoemission can induce an inverse sheath in a colder plasma, T_p will still substantially exceed T_{emit} in most conditions.

We see that for $T_R > 1$, $N_e^{\text{wall}} > N$. So the electron density in the inverse sheath increases toward the wall. [While this does not prove that the increase is monotonic, monotonicity can be shown by evaluating $dN_e(\varphi)/d\varphi$ analytically, confirming it is positive for $T_R > 1$ and using $dN_e/dx = dN_e/d\varphi \times d\varphi/dx$. We omit the calculation for brevity.]

In Fig. 4, N_e^{wall} increases with γ and with T_R. In the limit of $T_R \gg 1$, (14) reduces to

$$N_e^{\text{wall}} = N\gamma[1 + \text{erf}(\sqrt{\ln \gamma})]. \tag{15}$$

Because usually $\gamma < 2$ for SEE [23], and $N_e^{\text{wall}} < 2N\gamma$ via (15), this puts an upper bound on N_e in an inverse sheath of $\sim 4N$.

A useful approximation of the inverse sheath structure can now be derived. The preceding analysis shows that the electron density in an inverse sheath always exceeds N, but not by more than a factor of a few. Therefore, given that N_{ion} is zero, it is reasonable to approximate the total charge in the inverse sheath as a flat profile, with constant density $-N$. Poisson's equation in the sheath is then approximately

$$\frac{d^2\varphi(x)}{dx^2} = \frac{eN}{\varepsilon_0}. \tag{16}$$

Setting the origin $x = 0$, $\varphi = 0$ at the sheath edge, assuming zero electric field at the edge, and integrating (16) twice gives a parabolic potential profile,

$$\varphi(x) = \frac{eN}{2\varepsilon_0}x^2. \tag{17}$$

Applying the boundary condition $\varphi(x_{\text{wall}}) = \Phi_{-1}$ at the wall, we can determine the location of the wall relative to the sheath edge from (17). This gives a simple estimate of the spatial size of an inverse sheath Δx_{inv},

$$\Delta x_{\text{inv}} \approx \sqrt{\frac{2\varepsilon_0 T_{\text{emit}} \ln \gamma}{e^2 N}}. \tag{18}$$

Equation (18) is a robust estimate for SEE-driven inverse sheaths. Even if $N_e(x)$ were to increase by a factor of 4 from the sheath edge to the wall, Δx_{inv} from (18) would still be accurate within better than a factor of 2. For thermionic emitting surfaces, the equivalent γ can be much larger (e.g., up to 52 in Ref. [10]), so that $N_e^{\text{wall}} \gg N$. An improved estimate for Δx_{inv} is obtainable by using $\frac{1}{2}N_e^{\text{wall}}$ instead of N in (18), where N_e^{wall} is calculated from (14).

Another important property of the inverse sheath is that its spatial size is very small. To see this quantitatively, we compare to a common estimate of a nonemitting classical Debye sheath size $\Delta x_D \approx 10\lambda_D$ (from p. 76 of Ref. [1]), where $\lambda_D = (\varepsilon_0 T_p/e^2 N)^{1/2}$ is the Debye length. Dividing Δx_{inv} from (18) by $10\lambda_D$ gives

$$\frac{\Delta x_{\text{inv}}}{\Delta x_D} \approx \sqrt{\frac{T_{\text{emit}} \ln \gamma}{50 T_p}}. \tag{19}$$

So because usually $T_p \gg T_{\text{emit}}$, and because of the $(50)^{1/2}$ factor, it follows that $\Delta x_{\text{inv}} \ll \Delta x_D$. We conclude that the inverse sheath arising when $\gamma > 1$ is far smaller than the classical sheath that would arise if the same plasma (same N and T_p) were facing a nonemitting material ($\gamma = 0$). The inverse sheath is also far smaller than the SCL sheath that could arise in theory for the same $\gamma > 1$. (The structure of the ion-rich layer of the SCL sheath is similar to that of the nonemitting sheath, so it has a similar size scale.)

As a final comment we can test the accuracy of the equations from this inverse sheath model by checking limits. As $\gamma \to 1$ from above, $N_e^{\text{wall}} \to N$ in (14), $\Phi_{-1} \to 0$ in (11), and $\Delta x_{\text{inv}} \to 0$ in (18), as should be expected because no sheath structure is needed if $\gamma = 1$ exactly. For $\gamma < 1$, the inverse sheath solution should break down. Indeed, with $\gamma < 1$, N_e^{wall} and Δx_{inv} are undefined, and $\Phi_{-1} < 0$ in (11), contradicting the premise that the wall potential exceeds the sheath edge potential.

D. Effect of nonzero ion temperature

The main reason for using $T_{\text{ion}} = 0$ in the model was for simplicity, and to show that the ions do not need to reach the wall when $\gamma > 1$. For nonzero T_{ion}, the inverse sheath solution still always exists when $\gamma > 1$. The key fundamental concept is that ions do not need to enter the sheath with a *flow velocity*. When there is no flow velocity at the inverse sheath edge, $N_{\text{ion}}(\varphi)$ decreases with increasing φ as the wall is approached. So because the electron density increases with increasing φ (Sec. III C), the charge between the edge and the wall is automatically negative. Hence the argument of Sec. III A that the inverse sheath solution exists self-consistently is valid for nonzero T_{ion}.

The mathematical model can be extended to account for thermal ions. Thermal ions will enter and reflect from an inverse sheath in the same way that thermal plasma electrons behave in a classical sheath. When $T_{\text{ion}} \ll T_{\text{emit}}$, the influence of ions is negligible, and the cold ion approximation is valid. For larger T_{ion}, the ions produce a significant charge density in

the inverse sheath, which will cause the sheath spatial size to increase.

Nonzero $T_{\rm ion}$ will also produce a nonzero $\Gamma_{\rm ion}$. This will cause Φ_{-1} to increase, but only by a small amount. If the ions approaching the wall are half Maxwellian at the sheath edge, the flux in terms of Φ_{-1} is

$$\Gamma_{\rm ion} = \frac{N\sqrt{\frac{2T_{\rm ion}}{m_{\rm ion}\pi}}\exp\left(\frac{-e\Phi_{-1}}{T_{\rm ion}}\right)}{1+\mathrm{erf}\left(\sqrt{\frac{e\Phi_{-1}}{T_{\rm ion}}}\right)}. \tag{20}$$

In (20), it was assumed that the *total* ion density at the sheath edge is N. So the denominator gives the fraction of ions approaching the wall, accounting for wall losses and the return of ions reflected in the sheath. Now if $\Gamma_{\rm ion}$ is included in the zero-current condition (9) it can be shown that the (transcendental) solution for Φ_{-1} becomes

$$e\Phi_{-1} = T_{\rm emit}\left[\ln\gamma + \ln\left(\frac{1+\frac{\sqrt{\frac{T_{\rm ion}}{T_{\rm emit}}}\sqrt{\frac{m_e}{m_{\rm ion}}}\exp\left(\frac{-e\Phi_{-1}}{T_{\rm ion}}\right)}{1+\mathrm{erf}\left(\sqrt{\frac{e\Phi_{-1}}{T_{\rm ion}}}\right)}}{1-\frac{\sqrt{\frac{T_{\rm ion}}{T_{\rm p}}}\sqrt{\frac{m_e}{m_{\rm ion}}}\exp\left(\frac{-e\Phi_{-1}}{T_{\rm ion}}\right)}{1+\mathrm{erf}\left(\sqrt{\frac{e\Phi_{-1}}{T_{\rm ion}}}\right)}}\right)\right]. \tag{21}$$

The second term in the right-hand side of (21) is a positive term appearing due to the nonzero $T_{\rm ion}$. But because of the smallness of $m_e/m_{\rm ion}$ ($<10^{-3}$), it follows that the argument of the logarithm is very close to unity for most realistic values of $T_{\rm ion}/T_{\rm emit}$ and $T_{\rm ion}/T_{\rm p}$. (The unknown factors exp( ) and $1/[1+\mathrm{erf}(\,)]$ serve to further push the argument closer to unity.) Overall, we see that the thermal ions will not increase Φ_{-1} significantly compared to the $T_{\rm ion}=0$ solution unless γ is also very close to unity.

IV. IMPLICATIONS OF THE INVERSE SHEATH EFFECT

The sheath physics for strongly emitting surfaces is relevant to a diverse variety of systems including those mentioned in the Introduction. The inverse sheath would have important implications for the PWI because it is fundamentally different in several ways from classical and SCL sheaths.

One important aspect of the inverse sheath regime is that the ion-induced sputtering is negligible. This could be significant in many systems, particularly fusion machines. It has long been proposed that deliberate use of emitting wall materials could benefit future tokamaks such as ITER [25], the basis being that emission reduces the amplitude of classical sheaths, thereby reducing the impact energy of ions. The phenomenon of space charge saturation was thought to limit the maximum benefit of the emission, as $|\Phi_{\rm f}|$ was assumed to never fall below the SCL limit [25]. However, in light of the inverse sheath effect, it should be possible to fully eliminate ion sputtering because $\Gamma_{\rm ion}$ drops to zero. While $\Gamma_{\rm ion}$ will not be negligible if the ions are hot, the sputtering will still be dramatically reduced because there is no ion acceleration to the wall.

Another key consequence of $\Gamma_{\rm ion}=0$ is that the wall is no longer a plasma sink. In general, the state of a plasma depends crucially on the balance between the ion-electron generation and losses. In the classical and SCL regimes, the loss rate of charged particles to the boundaries is a fixed value (essentially independent of γ) determined by the Bohm velocity and plasma density at the sheath edge. But for $\gamma>1$ in the inverse sheath regime, the loss rate of ions and electrons to the boundaries is zero. No neutrals will recycle back to the plasma from the walls. Although there will be some charge loss if $T_{\rm ion}>0$, the loss rate is always much smaller in the inverse sheath regime compared to the classical and SCL regimes.

A possible drawback of the inverse sheath regime is that the electron energy flux to the wall and the corresponding plasma energy loss are very large. In general, emission causes enhanced wall energy flux because the extra plasma electrons which must reach the wall to compensate the emission usually have much larger temperature than the emitted electrons that enter the plasma ($T_{\rm p}\gg T_{\rm emit}$). Some authors have stated that the SCL regime is "considered the maximum plasma interaction of ambient plasmas with the surrounding boundary [15]" because $\Gamma_{\rm p}$ is assumed to never exceed its value at space charge saturation. But in the inverse sheath regime, all plasma electrons are unconfined and the wall faces the full thermal influx.

The difference between $\Phi_{\rm f}>0$ and $\Phi_{\rm f}<0$ is significant in any application where the surface potentials are important. For example, when emissive probes are used to measure space potential in plasmas, it is usually assumed that the sheath is SCL. The space potential is taken to be about $1T_{\rm p}$ above the measured floating potential of the probe [11]. But if the probe were in the inverse sheath regime, the space potential would fall below the measured floating probe potential. Another situation where surface potentials are important is in differentially charged spacecraft. Strong emission is possible for spacecraft surfaces in contact with hot background plasmas and/or intense sunlight [9].

Although we treated floating walls formally in Sec. III, the inverse sheath effect is also relevant to current-carrying walls. When a plasma is bounded between mutually biased walls, the plasma potential itself is determined self-consistently by the condition that the total current out of the plasma is zero globally. If the walls emit sufficiently strong electron currents, then the wall potentials can all exceed the plasma potential. For instance, consider a planar plasma between two conducting walls biased to equal potentials (that is, both walls have the same Φ relative to the plasma). Let one wall emit a flux $\Gamma_{\rm emit}$ and the other wall be nonemitting. For $\Gamma_{\rm emit}=0$, the walls have some $\Phi<0$. For larger $\Gamma_{\rm emit}$, Φ becomes less negative. For some critical $\Gamma_{\rm emit}$, the emitting wall sheath becomes SCL. General theories may assume that the walls remain at $\Phi<0$ for arbitrarily large $\Gamma_{\rm emit}$ as the additional emission is limited by the virtual cathode [20]. However, there will be a critical $\Gamma_{\rm emit}$ beyond which both walls can have $\Phi>0$ with inverse sheaths. The total current between the walls will still be limited but not in the same physical way.

V. WHICH SHEATH STRUCTURE WILL APPEAR IN PRACTICE UNDER STRONG EMISSION?

A. Theoretical considerations

Both the SCL sheath and inverse sheath are legitimate theoretical solutions to the strong emission problem. Because the two regimes have drastically different properties as discussed in Sec. IV, it is instinctive to ask which sheath will

appear in practice at floating surfaces. A variety of theoretical arguments could be made in favor of either sheath.

For instance, the inverse sheath configuration consisting of a single negative charge layer shielding the positively charged wall [Fig. 2(e)] is simpler than the SCL configuration consisting of a negative charge layer, a positive charge layer further inward, and an ion-accelerating presheath [Fig. 2(d)]. In addition, it may seem more natural from an electrostatics viewpoint for ions to be repelled from a positively charged wall than drawn to it. The inverse sheath is also a lower-potential-energy configuration.

On the other hand, it could be argued that a SCL sheath should exist at a wall with $\gamma > 1$ as long as γ was below unity at some time in the past. A wall contacting a hot laboratory plasma that started from a colder initial state would transition past $\gamma = 1$ as the temperature is raised to its equilibrium value. An analogy for thermionic emission is when an emissive probe is inserted into a plasma before it is heated to emit. In these cases, a SCL sheath with a presheath and a dip must already exist before γ crosses unity, so the sheath could easily remain SCL after the transition. But this argument does not guarantee that a SCL sheath would persist indefinitely. Experiments have shown that potential dips are spontaneously destroyed by accumulation of slow ions produced from ion-neutral collisions or charge exchange with slow neutrals [10].

B. Past empirical studies

Because theoretical arguments alone cannot determine which sheath will form under strong emission, direct empirical studies would be valuable. Unfortunately, probing the full structure of the space potential in sheaths is difficult due to their small spatial size, and resolving the much smaller region where the emitted electrons reflect back to the wall in an emissive sheath is formidable. So there are few high-resolution probe measurements of the space potential near emitting surfaces in the literature.

Measurements of space potential showing a virtual cathode dip structure near a surface with SEE were reported recently by Li *et al.* [26]. But the surface was electrically biased below the plasma potential, not floating as we wish to study here. Intrator *et al.* measured space potential near a floating thermionic emitting cathode [10]. In Fig. 6 of the paper, it was found that when the emission was strongest, the cathode floated more positively than the background plasma, as in an inverse sheath regime, but the potential profile was also nonmonotonic with a dip resembling a SCL sheath. So the result cannot be classified exclusively as one of the planar sheaths in Fig. 1. Of course, in experiments the sheath physics is often more complex than one-dimensional (1D) models can explain. The potential distribution in the cathode region in Ref. [10] was shown to be influenced by 3D nonuniformities and by the presence of an ion beam injected from the plasma source region.

Another way one can empirically study plasma-wall interaction with emission is by particle-in-cell simulation. Particle simulation allows maintaining a simple plasma in one spatial dimension, measuring the potential distribution noninvasively, and directly tracking the emitted electrons, so that fundamental sheath physics can be analyzed closely.

In most particle simulation studies of PWI, a plasma is produced at a "source" boundary in front of the "collector" (wall) [13,14,27,28]. Ions and electrons are injected into the plasma domain at the same rate to maintain global neutrality. Because the ions and electrons have different velocity distributions, a non-neutral charge distribution forms near the source, creating a potential drop called a "source sheath." The source sheath is not caused by plasma interaction with the collector, which could be arbitrarily far from the source. But the source sheath accelerates ions toward the collector, so that the true plasma source facing the collector has drifting ions. This type of setup can artificially distort the physics of the $\gamma > 1$ problem because it forces ions to flow to the wall.

Schwager presented the seminal simulation-based study of PWI with electron emission [13]. In Fig. 9 of the paper, a SCL collector sheath with a dip was observed in a simulation with $\gamma = 1.5$. But in the same potential profile near the source boundary was an ion-accelerating source sheath of amplitude $\sim$30 times larger than the dip. More recently Zhang *et al.* simulated PWI with strong SEE to investigate interesting sheath oscillation effects [29]. In the simulation the ions were modeled as a spatially uniform background density flowing to the wall at a fixed velocity set to the Bohm velocity.

Overall, it is not yet known empirically what the sheath structure looks like at strongly emitting floating surfaces where ions are not directed toward the surface by an external mechanism (i.e., a mechanism other than the PWI). So here we will simulate a full bounded plasma system where the charged particles, and their temperatures, are sustained naturally within the plasma itself, and no ion beams are produced. That way ions will flow to the walls if and only if they "need" to.

C. Simulation of a full-scale plasma bounded by walls with $\gamma > 1$

As a simple yet realistic system, we will simulate a bounded planar plasma with a uniform background $E \times B$ field; see Fig. 5(a). A planar system is ideal for our study because the surface geometry will not affect the sheath physics. The $E \times B$ background field will serve as a natural heating mechanism for the plasma electrons; it does not (directly) affect the sheath physics either because it does not alter particle velocities normal to the walls. An electrostatic direct implicit particle-in-cell code for this configuration was produced by Sydorenko [30]. It has been applied for modeling Princeton Plasma Physics Laboratory (PPPL) Hall thruster (HT) plasmas [31,32]. The simulation results provided valuable insight into the experimental measurements discussed in a recent review paper by Raitses *et al.*; see Ref. [33].

A theoretical analysis of the plasma properties and the wall fluxes as a function of the controllable simulation parameters is given in Ref. [32] for applications to HTs. However, the theory assumes that $\Phi_f < 0$ sheaths always exist at the walls. When the electron $E \times B$ drift energy exceeds a threshold value, the electrons incident on the walls eject more than one secondary on average. The system enters the inverse sheath regime, where the physics behind the plasma properties and the PWI drastically changes. A detailed theoretical explanation of the transition between the two regimes is given in Ref. [34]. But in Fig. 1 of Ref. [34] the inverse sheath structure was unclear. The simulation spatial grid, which was suitable for

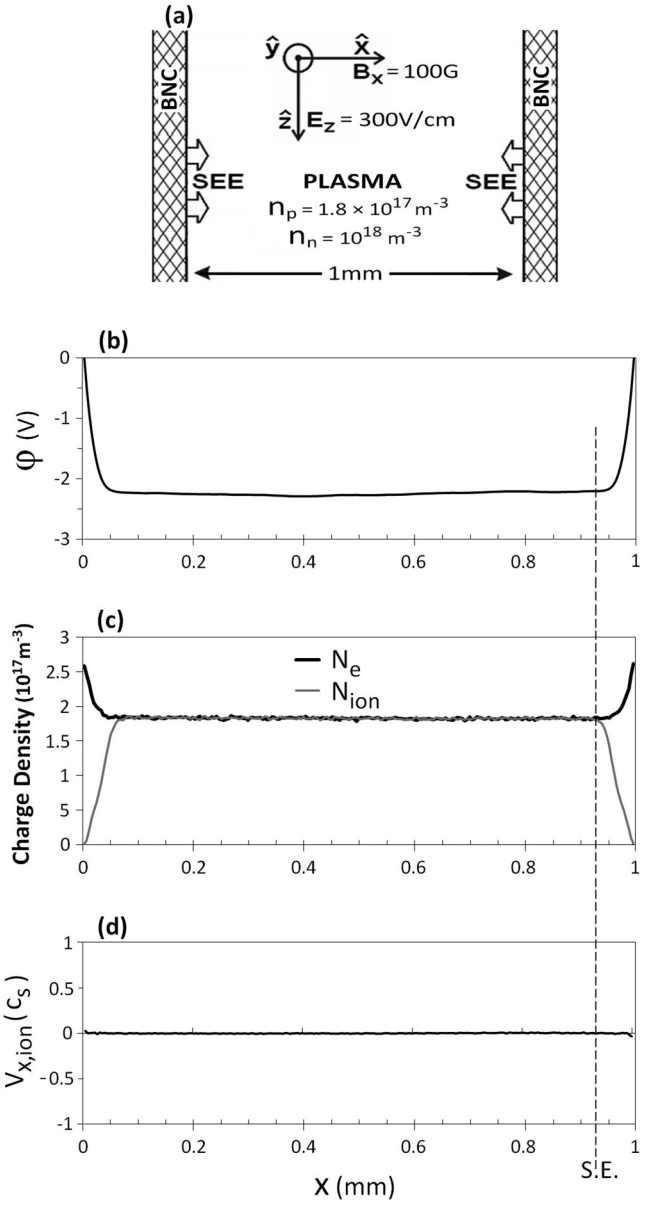

FIG. 5. (a) Schematic of the simulation model with the main discharge parameters for the current run listed. (b) The electrostatic potential relative to the right wall. (c) Charge density profiles. (d) Ion velocity normal to the walls. $V_{x,\mathrm{ion}}(x)$ is the mean velocity of the ions in the two cells neighboring each grid point, normalized to $c_s = 2053$ m/s, the ion sound speed calculated from the electron distribution over v_x in the simulation. Note that the plots are high resolution; the grid spacing 4.4 μm is more than ten times smaller than the sheath size. "S.E." marks the right sheath edge.

resolving classical Debye sheaths, could not resolve the much smaller inverse sheath. The ~1 V amplitude inverse sheath was also obscured by strong ~5 V potential fluctuations caused by plasma waves.

Here in Fig. 5 a simulation with enhanced grid resolution and time-averaged data is presented in order to reveal the true steady-state sheath physics. The discharge behaves as follows. Secondaries are emitted from the walls with a low-energy thermal distribution. The secondaries that overcome the inverse sheath propagate across the plasma in the x direction while undergoing $E \times B$ drift motion in the y-z plane. With $E_z = 300$ V/cm and $B_x = 100$ G, the drift energy oscillates between 0 and 102 eV. So the electrons carry high energies upon impact at the other wall, sufficient to induce a net SEE coefficient of 1.3 from the boron nitride ceramics material. Electron collisions are included in the model but their effects are negligible here. With a (xenon) plasma density $n_\mathrm{p} = 1.8 \times 10^{17}$ m^{-3} and a (uniform) neutral background density $n_\mathrm{n} = 10^{18}$ m^{-3}, it turns out that the transit time of the unconfined electrons from wall to wall is less than the average time between collisions of all types. When E_z/B_x is lower, classical sheaths confine most electrons in the plasma interior and the neutral, Coulomb, and turbulent collisions are crucial to the plasma properties [32]. In the inverse sheath regime, it is the ions that are confined by the sheaths. In the run presented, ions were found to come to a roughly Maxwellian equilibrium with uniform temperature $T_\mathrm{ion} = 0.5$ eV. (This was not controlled by the user; ions suffer no collisions and respond only to the plasma's self-generated electric field normal to the walls.)

Figure 5 shows the profiles of $\varphi(x)$, $N_e(x)$, $N_\mathrm{ion}(x)$, and $V_{x,\mathrm{ion}}(x)$ over the plasma domain. The plasma width was set to 1 mm so that the plasma and sheath regions could be resolved with a reasonable computation time. There are 229 grid points spaced uniformly 4.4 μm apart. The plotted profiles are averages of 17 snapshots taken 25 ns apart in order to filter out fluctuations from plasma waves and instabilities that appear in the simulations [34] (periodic and random fluctuations average out to zero long term).

D. Analysis of the simulation profiles

Usually for a plasma between two walls [1], N_e(x) and $\mathrm{N_{ion}}(x)$ decrease by a factor of about 2 from the plasma center to the sheath edges because of the presheaths. There is a substantial ion flow velocity throughout the plasma domain; $V_{x,\mathrm{ion}}(x)$ increases from zero at the plasma center to $\sim c_\mathrm{s}$ (ion sound speed) at the sheath edges. The potential $\varphi(x)$ has a local maximum at the center and is positive relative to the walls everywhere between the two sheath edges. These presheath properties should remain present with secondary emission under the conventional assumption that Φ_f is negative for all emission intensities. The properties are indeed observed for simulations with $\gamma < 1$ using the same simulation model [32].

But the profiles in Fig. 5 sharply differ from conventional plasma-wall interactions. There is clearly no ion-accelerating presheath structure in the system. $N_e(x)$ and $N_\mathrm{ion}(x)$ are flat between the two sheath edges. The ion mean velocity $V_{x,\mathrm{ion}}(x)$ is negligible everywhere compared to c_s. The sheath regions consist not of a double charge layer but instead a single negative charge layer. From the sheath edges toward the wall, $N_e(x)$ and $\varphi(x)$ monotonically increase, and $N_\mathrm{ion}(x)$ monotonically decreases. The potential $\varphi(x)$ is negative and flat between the sheaths. Overall, the properties of the profiles match the characteristics of the inverse sheath regime predicted theoretically in this paper.

The inverse sheath's spatial width is 68 μm. This value is within a factor of 2 of the estimate $(2\varepsilon_0\Phi_{-1}/eN)^{1/2} = 37$ μm from (18) based on the flat charge density profile approximation, using $\Phi_{-1} = 2.2$ V and $N = 1.8 \times 10^{17}$ m^{-3}.

The underestimate is attributable to finite ion temperature. With $T_{ion} = 0.5$ eV, ions can penetrate a significant distance into the inverse sheaths, although very few can reach the wall as $\exp(-2.2/0.5) \approx 0.01$.

The value $\Phi_{-1} = 2.2$V cannot be calculated easily in terms of simulation parameters. First, the coefficient $\gamma = 1.3$ was not a set parameter but is determined self-consistently with the irregular plasma electron velocity distribution and wall SEE yield function. Also, the emission velocity distribution in the model is complicated. The "true secondaries" are emitted with an energy distribution $\sim w^{1/2}\exp(-w/T_{emit})$ and have a nonisotropic angular distribution [30]. We set T_{emit} to 5 eV (to make the inverse sheath larger and easier to resolve, while 2 eV is a more realistic value). There are also "nontrue" secondaries consisting of hot electrons that reflect or backscatter off the wall. The higher-energy secondaries are the main reason why $e\Phi_{-1}$ exceeds the estimate $T_{emit}\ln\gamma = (5\text{ eV}) \times \ln 1.3 = 1.3$ eV based on the Maxwellian assumption.

The author has conducted studies of the sheath structures in this simulation model as the parameters (E_z, B_x, and other conditions) are varied over a wide range. It turns out whenever $\gamma > 1$, inverse sheaths form at the walls. While it should also be possible for a SCL sheath to form, a SCL sheath has not yet been observed in steady state. So it seems the inverse sheath is the more natural solution, at least in this simulation configuration.

Interestingly, a nonmonotonic $\varphi(x)$ qualitatively similar to a SCL sheath does appear in some simulations, as shown previously in Fig. 3 of Ref. [35] by Sydorenko *et al*. However, it exists only briefly during an instability. It was later shown that the nonmonotonic $\varphi(x)$ appears because a classical sheath with a presheath exists initially, and then the "weakly confined electron" instability causes the wall charge to change from negative to positive before the heavy ions have a chance to respond (see Fig. 5 of Ref. [36] and the discussion therein). Hence the nonmonotonic $\varphi(x)$ is not a true SCL sheath as the corresponding charge density profiles cannot exist in steady state.

VI. CONCLUSION

A type of sheath structure that can appear in plasma systems with surfaces emitting strong secondary, thermionic, or photon-induced electron currents was described. Past theoretical models predicting that a nonmonotonic SCL sheath with positive plasma potential forms when $\gamma > 1$ rely on an assumption that ions always have to flow to the wall [12–15]. But when the emission exceeds a threshold intensity, the zero-current condition and the plasma shielding requirement can be maintained without ion flow to the wall. Relaxing the ion flow assumption at the sheath edge allows the inverse sheath solution.

In the inverse sheath regime, the potential $\varphi(x)$ monotonically increases from the sheath edge to a positively charged wall. Ions are repelled from the wall and the ion velocity is zero everywhere in the plasma. An analytical inverse sheath solution was derived for a general plasma-wall system where the plasma electrons and emitted electrons are Maxwellian with temperatures T_p and T_{emit}. The inverse sheath amplitude $e\Phi_{-1} = T_{emit}\ln\gamma$ and its spatial width, estimated as $\Delta x_{inv} = (2\varepsilon_0 T_{emit}\ln\gamma/e^2 N)^{1/2}$, are much smaller than those of a classical Debye sheath or SCL sheath.

There are few direct experimental measurements of emissive sheaths in the literature due to the difficulty of probing the small structures. A high-voltage Hall discharge where the SEE coefficient exceeded unity at the walls was simulated by the particle-in-cell method in order to test empirically whether a SCL or inverse sheath would form at the walls. It was found that inverse sheaths formed; ions were confined in the plasma, and there was zero ion flow throughout the domain. Although a past particle simulation study by Schwager reported formation of a SCL sheath at an emitting wall [13], that model had an artificial source sheath that accelerated ions to the wall.

The inverse sheath effect drastically alters how a plasma interacts with a wall. Most importantly, with zero ion flux, the sputtering and charged particle loss to the wall are eliminated. No presheath potential gradient exists to accelerate the ions. The distributions of potential, ion density, and electron density in the sheath and the plasma are much different in the inverse sheath regime compared to the classical and SCL regimes. The author hopes these results motivate future experimental studies of the sheath structure facing strongly emitting surfaces.

ACKNOWLEDGMENT

This work was supported by the U.S. Department of Energy under Contract No. DE-AC02-09CH11466.

[1] P. C. Stangeby, *The Plasma Boundary of Magnetic Fusion Devices*, Plasma Physics Series (IOP, Bristol, 2000).
[2] R. H. Cohen and D. D. Ryutov, Contrib. Plasma Phys. **44**, 111 (2004).
[3] K. U. Riemann, J. Phys. D **24**, 493 (1991).
[4] I. V. Tsvetkov and T. Tanabe, J. Nucl. Mater. **266**, 714 (1999).
[5] R. A. Pitts and G. F. Matthews, J. Nucl. Mater. **176**, 877 (1990).
[6] J. P. Gunn, Plasma Phys. Controlled Fusion **54**, 085007 (2012).
[7] Y. Raitses, D. Staack, A. Smirnov, and N. J. Fisch, Phys. Plasmas **12**, 073507 (2005).
[8] J. Pavlů, J. Šafránovká, Z. Němeček, and I. Richterová, Contrib. Plasma Phys. **49**, 169 (2009).
[9] E. C. Whipple, Rep. Prog. Phys. **44**, 1197 (1981).
[10] T. Intrator, M. H. Cho, E. Y. Wang, N. Hershkowitz, D. Diebold, and J. DeKock, J. Appl. Phys. **64**, 2927 (1988).
[11] J. P. Sheehan, Y. Raitses, N. Hershkowitz, I. Kaganovich, and N. J. Fisch, Phys. Plasmas **18**, 073501 (2011).
[12] G. D. Hobbs and J. A. Wesson, Plasma Phys. **9**, 85 (1967).
[13] L. A. Schwager, Phys. Fluids B **5**, 631 (1993).
[14] F. Taccogna, S. Longo, and M. Capitelli, Phys. Plasmas **11**, 1220 (2004).
[15] J. Seon, E. Lee, W. Choe, and H. J. Lee, Curr. Appl. Phys. **12**, 663 (2012).

[16] J. P. Sheehan, I. Kaganovich, N. Hershkowitz, and Y Raitses, http://homepages.cae.wisc.edu/~sheehan/sheehan_invitedTalk_icops2012.pdf.
[17] A. Dove, M. Horanyi, X. Wang, M. Piquette, A. R. Poppe, and S. Robertson, Phys. Plasmas **19**, 043502 (2012).
[18] C. A. Ordonez, Phys. Fluids B **4**, 778 (1992).
[19] T. Gyergyek, J. Kovačič, and M. Čerček, Phys. Plasmas **17**, 083504 (2010).
[20] I. Langmuir, Phys. Rev. **33**, 954 (1929).
[21] V. L. Sizonenko, Sov. Phys. Tech. Phys. **26**, 1345 (1981).
[22] A. I. Morozov and V. V. Savel'ev, Plasma Phys. Rep. **33**, 20 (2007).
[23] C. A. Ordonez and R. E. Peterkin, J. Appl. Phys. **79**, 2270 (1996).
[24] M. Kaminsky, *Atomic and Ionic Impact Phenomena on Metal Surfaces* (Academic Press, New York, 1965).
[25] M. J. Embrechts and D. Steiner, in *Proceedings of the IEEE 13th Symposium on Fusion Engineering, Knoxville, TN, 1989*, edited by M. S. Lubell, M. B. Nestor, and S. F. Vaughan (IEEE, New, York, 1989), Vol. 1, pp. 538–541.
[26] W. Li, J. X. Ma, J. Li, Y. Zheng, and M. Tan, Phys. Plasmas **19**, 030704 (2012).
[27] A. Bergmann, Nucl. Fusion **42**, 1162 (2002).
[28] D. Tskhakaya and S. Kuhn, Contrib. Plasma Phys. **40**, 484 (2000).
[29] F. Zhang, D. Yu, Y. Ding, and H. Li, Appl. Phys. Lett. **98**, 111501 (2011).
[30] D. Sydorenko, Ph.D. thesis, University of Saskatchewan, 2006.
[31] D. Sydorenko *et al*., Phys. Plasmas **13**, 014501 (2006).
[32] I. D. Kaganovich, Y. Raitses, D. Sydorenko, and A. Smolyakov, Phys. Plasmas **14**, 057104 (2007).
[33] Y. Raitses *et al*., IEEE Trans. Plasma Sci. **39**, 4 (2011).
[34] M. D. Campanell, A. V. Khrabrov, and I. D. Kaganovich, Phys. Rev. Lett. **108**, 255001 (2012).
[35] D. Sydorenko, I. Kaganovich, Y. Raitses, and A. Smolyakov, Phys. Rev. Lett. **103**, 145004 (2009).
[36] M. D. Campanell, A. V. Khrabrov, and I. D. Kaganovich, Phys. Plasmas **19**, 123513 (2012).